

Lithium-ion batteries diagnosis toward second-use prognosis

Coron Eddy^{1,3}, Geniès Sylvie¹, Delaille Arnaud², Thivel Pierre-Xavier³

¹*Univ. Grenoble Alpes, CEA, LITEN, DEHT, LAP, F-38000 Grenoble, France - eddy.coron@cea.fr*

²*Institut national de l'énergie solaire. 50, avenue du lac Léman 73375 Le Bourget-du-Lac Cedex*

³*Univ. Grenoble Alpes, Univ. Savoie Mont Blanc, CNRS, Grenoble INP, LEPMI, 38000 Grenoble, France*

Summary

In order to enable the second-use of lithium-ion batteries (LIB) used in electric vehicles, it is necessary to better understand the degradation mechanisms that lead to their capacity and power losses. Based on voltage curves and pulse power characterisation, this work aims to develop a fast and comprehensive diagnosis method. Some 18650 commercial LIB made of two different active materials were aged following different procedures leading to various ageing mechanisms. The degradations were confirmed using *post-mortem* analysis. At the end distinctive SOHs in accordance with the internal degradation mechanisms of the cells via the non-invasive diagnosis technique could be given.

Keywords: Prognosis, Diagnosis, Battery SOH, Battery ageing, Second-life battery

1 Introduction

One of the last barrier for the mass-market adoption of LIB powered vehicles is their cost. In this context, reusing the batteries for a second life is a solution to improve their competitiveness. The LIB that do not meet the requirements of electric vehicles anymore could be reused for stationary applications, i.e. frequency regulation, peak shaving, on-grid and off-grid storage for renewable energies. It is believed that these secondary batteries will become competitive enough to be used instead of new Li-ion or lead-acid cells for this kind of applications that do not need a very high power density. However, there is still one uncertainty: how long these secondary batteries can fulfill their requirements? The shift-point between first life (in automotive application) and second life corresponds to a capacity fading of approximatively 20-30% [1], because at this point the driving range becomes too low. Then, the duration of the second life depends on degradation mechanisms induced by driving and storage conditions of the LIB during its first life. Typical degradation mechanisms for LIB are the loss of active material (LAM), loss of lithium inventory (LLI) and lithium plating. The aim of the work is to implement a fast and efficient diagnosis technique for retired LIB in order to assess which degradation mechanism had affected their capacity. The relation between the detected degradation and the second-use lifetime is tested via a comprehensive experiment plan. 18650-format commercial lithium-ion cells were aged following different procedures, leading to favored different

degradation mechanisms. Then, some cells were dismantled to analyze their ageing (via *post-mortem* analysis of the internal components), while others were over-aged to determine their second-use lifetime.

2 Diagnosis of LIB degradation mechanisms

2.1 Degradation mechanisms

The electric vehicles LIB are used under various temperature and current conditions. Moreover, the manufacturers use many various electrode materials, and these materials react differently depending on the ageing conditions. Out of a long list of potential degradation mechanisms, three of them are usually highlighted in the literature[2] [3] and reported below:

- The loss of active material affects both electrodes. It can be caused by mechanical stress (mainly occurring at the negative electrode), dissolution of transition metal and crystalline phase modification (positive electrode).
- The loss of lithium inventory is mainly caused by the growth of a Solid-Electrolyte Interphase (SEI) at the carbon-based negative electrode. The concomitant decomposition of the electrolyte occurs onto the electrode, usually when the state of charge (thus, the voltage) and the temperature are high.
- The lithium plating corresponds to the formation of a metallic lithium deposition on the negative electrode. Low temperature and/or high charging current usually lead to this dramatic degradation mechanism. It is also a type of loss of lithium inventory, but it is worse as this usually degrades the safety of the cell. As the plated negative electrode cannot anymore contribute to the lithium ions exchange, the current density increases elsewhere on the negative electrode, leading to generalized lithium plating within a small number of cycles.

Figure 1 summarizes the degradation mechanisms affecting lithium-ion batteries.

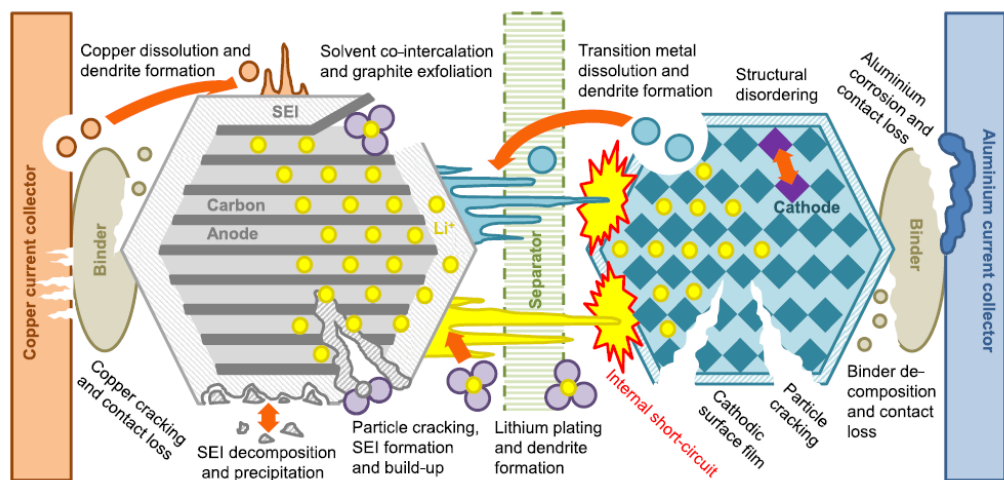


Figure 1: Schematic representation of the numerous potential degradation mechanisms of a LIB.[2]

2.2 Diagnosis techniques

It is required by the end-user that the diagnosis technique is as fast as possible, non-destructive and cost-effective. Thus, electrochemical data based on voltage curves can be analysed to highlight the degradation of an electrode, the loss of lithium and the resistances increase. These data will be processed in order to build a two electrodes model, in which the electrodes potentials are deduced from the full cell data [2].

2.2.1 Incremental capacity analysis (ICA)

We have applied the Incremental Capacity Analysis (ICA) method that is commonly used to track the electrochemical properties from the battery cell[4]. The voltage curves are processed into differential voltage curves in order to highlight the voltage plateaus. These plateaus correspond to the phase transition within the electrode materials, occurring during the lithiation/delithiation processes. To obtain these curves, it is necessary to calculate the amount of charge exchanged between two close voltage values. These $\frac{dQ}{dV}$ are usually plotted versus voltage, as depicted in Figure 2 a). Thus, the plateaus of the $V(Q)$ curves are highly visible as they are peaks on the $\frac{dQ}{dV}$ plot. It is also possible to represent its inverse, i.e. the voltage variations divided by the charge. The resulting $\frac{dV}{dQ}$ curves show valleys corresponding to the SoC range of the plateaus, as the Figure 2 c) shows.

It has to be noted that this technique is dependent on the cell chemistry: as the electrode materials have different voltage curves during lithiation and delithiation processes, the comparison of different cells with different chemistries and/or different design/loading ratios is not relevant.

Another important aspect is the fact that a relative low charging/discharging current rate is necessary. The influence of current rates has been shown and will be discussed in this document.

The values of the sampling dV (or dQ) are also fundamental. Signals are highly dependent on this value; it makes no sense to compare differential analysis processed with different dV values. Consequently, the voltage and current resolution of the galvanostat have to be set mindfully.

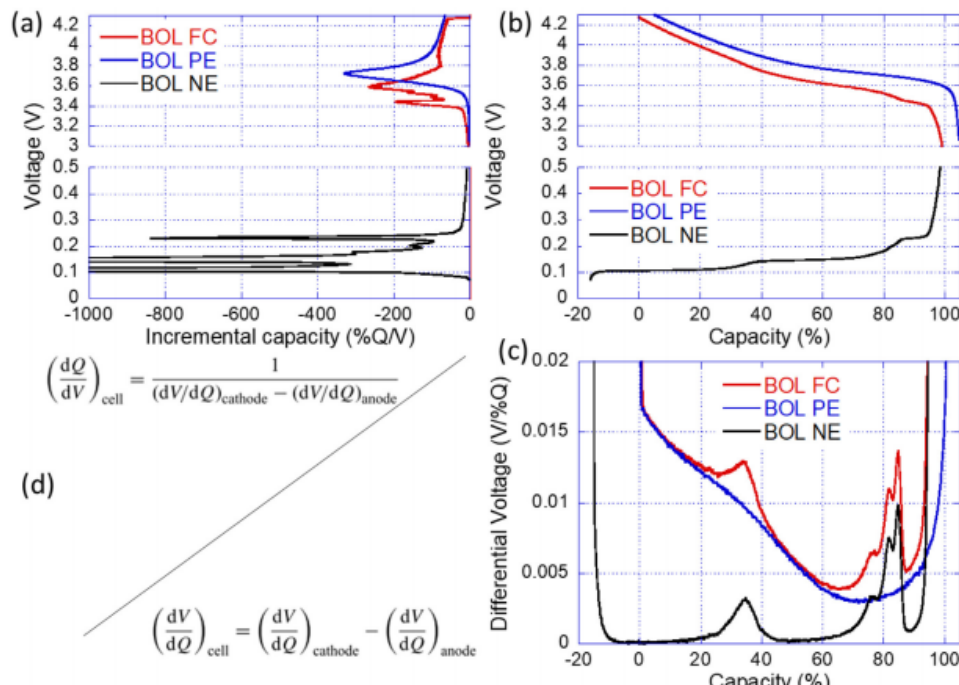


Figure 2: a) $\frac{dQ}{dV}$ curve b) $V=f(Q)$ c) $\frac{dV}{dQ}$ curve for the negative electrode (black), positive electrode (red) and full cell (blue). d) Associated equations BOL stands for beginning of life.[5]

These curves can be used qualitatively: they offer a better resolution than the $Q(V)$ curve, as Figure 2 a-c) illustrates. This way, using the $\frac{dQ}{dV}(V)$ curve, it becomes easier to claim that a same degradation mechanism affected two different cells (from the same reference). On the contrary, this method also helps to claim that two identical cells suffered from different ageing mechanisms.

To assess some quantitative information about the degradations of the cells, these data are also useful. By modelling the potential of both electrodes, it is possible to follow these degradations. Loss of active material will result in the shortening of the concerned electrode V(Q) curve, thus modifying the $\frac{dQ}{dV}(V)$. Loss of lithium inventory leads to a slippage of the potential curves, as a part of them cannot be used anymore, because of the lack of exchangeable lithium ions. Calculations needed for the reconstruction of the potential curves are shown in Figure 2 d). However, it is not relevant to describe the variation of the differential voltage curves, as it is, once again, dependant on the cell.

2.2.2 Pulse Power Characterisations

Another fast diagnosis technique is based on pulse power tests. This usually consists of a current step that typically last several seconds. The voltage response is analysed in order to calculate a pseudo-resistance. The results depend on the pulse time length, the constant current value, the temperature and the SOC. The pseudo-resistance is a combination of several resistance contributions:

- R_{ohm} stands for the ohmic resistance, mainly dependant on the ionic conductivity of the electrolyte and on the electronic conductivity of the current collectors and active materials. This contribution is not dependant on the state of charge (SoC).
- R_{CT} , the charge transfer resistance, describes the transfer of the lithium from the electrolyte to the electrode and vice-versa.
- R_p , the polarisation resistance, which corresponds to the lithium diffusion within the active material

These contributions are difficult to deconvolute using pulse power characterisations but they have different characteristic time constant, as the Figure 3 depicts: the ohmic resistance could be calculated after a very short time while it needs more time under the current pulse to determine the polarisation resistance. Thus, we could figure that a longer pulse helps to determine the polarisation resistance. However, it has to be considered that the pulse duration may also affect the results as the SoC of the battery could be modified. In order to improve the measurement, it is also recommended to use relative high current amplitude, as it will involve a higher voltage response, thus a better signal/noise ratio.

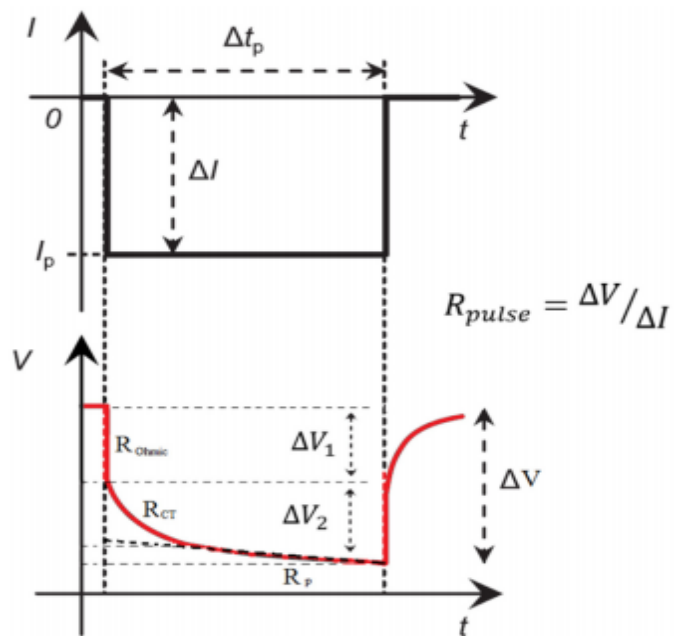


Figure 3: Schematic voltage response to a current step. The contributions of the ohmic resistance, charge transfer resistance and the polarisation resistance are indicated./5/

3 Methods

3.1 Ageing of the cells

Two different cell references, corresponding to distinct electrode compositions were studied. The first reference is representative of electric vehicles cell currently in use, as its positive electrode is a blend of NMC and LMO. A second reference was chosen to investigate the properties of a recent technology, embedding a nickel-rich positive electrode, which faces a silicon-doped negative electrode. The cells characteristic are given in the table 1.

These cells were aged following different procedures, favouring different degradation mechanisms. The procedures are described in the table 2. Different procedures including calendar ageing and other temperature conditions are currently under investigation and will be presented in a further work.

Table 1: Cells characteristics

	Positive electrode	Negative electrode	Release	Capacity (Ah)
Ref#1	NMC(111)+LMO	graphite	2011	2,1
Ref#2	NMC(811)	graphite+silicium	2014	3,5

Table 2: Ageing procedures

Procedure	C-rate / SoC (%)	Temperature (°C)	Targeted main degradation mechanism
Cycling 1	1C	25	LAM
Cycling 2	1C	0	Lithium plating

In order to characterise these cells along cycling, a check-up procedure was implemented. As described in the previous section, it was necessary to include low current charge and discharge steps, allowing the calculation of differential curves. Moreover, current pulses in charge and discharge are added, for 10 values of SoC varying from 0 to 100%. The amplitude of these pulses are 1C in charge and -2C in discharge, to meet the manufacturer requirements as well as reduced incertitude. Figure 4 describes the whole check-up procedure, including variations of the current, voltage and temperature of the cell:

- Step 1 is a residual discharge.
- Step 2 is the C/10 cycle.
- Step 3 consists of two C/2 cycles.
- Step 4 are 1C charge pulses and C/2 inter-pulses charges.
- Step 5 are -2C discharge pulses and -C/2 inter-pulses discharges.
- Step 6 is a 50% SOC charge.

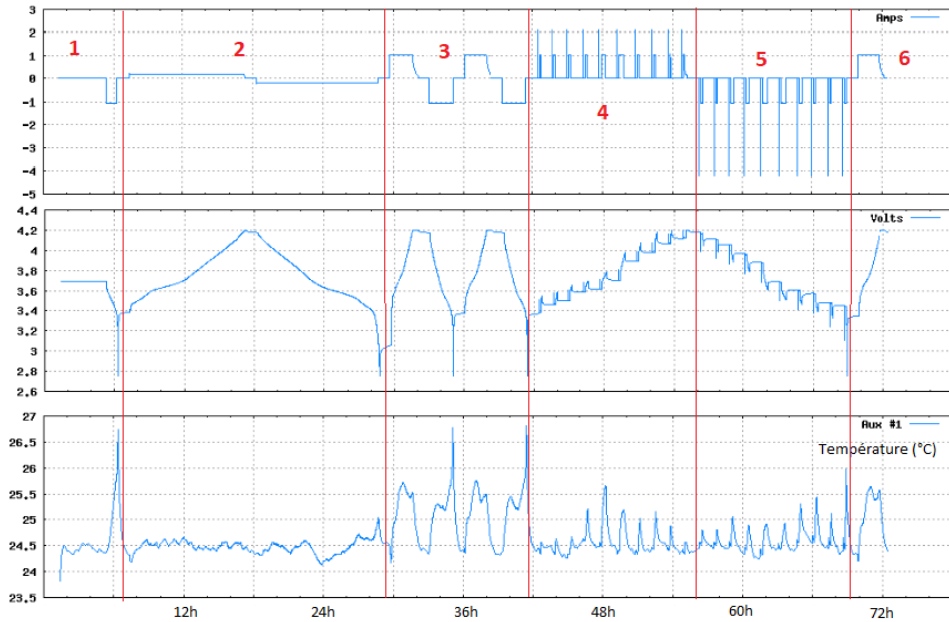


Figure 4: Current, voltage and temperature variations of a cell during a check-up.

3.2 Post-Mortem materials analysis

Once the cell lost 20% of their initial capacity, some of them were dismantled in an argon-filled glove box. Their electrodes were sampled and analysed using scanning electron microscopy (SEM) after rinsing in DMC and drying.

3.3 Post-Mortem electrochemical analysis

The electrodes collected from the dismantled commercial cells also allowed producing some half coin-cells. Metallic lithium is used as negative electrode, as its potential remains very stable during both charge and discharge of the commercial cell electrode, as long as the current is low enough. The electrode voltage curve is obtained via this technique.

Coin-cells were manufactured with fresh cells electrodes as well as aged cells electrodes. These half coin-cells allows quantifying the loss of active material of each electrode, as well as loss of lithium inventory. The cells were fully discharged before opening, following a constant current procedure with a C/10 rate, followed by a constant voltage step at the cut-off voltage, until the current dropped under a C/50 rate.

By manufacturing a “positive” half coin cell, using a 14mm diameter disk of the positive electrode versus a metallic lithium foil, and by lithiating this electrode once again, it is possible to estimate the part of “empty locations”. That means that some lithium ions are lost, either by the SEI growth or by metallic lithium plating, and these ions are thus irreversibly consumed and cannot be anymore be used to lithiate the positive electrode. Thus, the first lithiation after manufacturing of the positive electrode half coin-cell gives an indirect idea of the amount of lost lithium ion.

4 Results

4.1 Ageing and *Ante-Mortem* results

4.1.1 Capacity fade tendencies

The capacity fade of these commercial cells is showed on the Figure 5. The end of the ageing was chosen to be at a SOH of 80%. It is particularly striking to see that the Ref#2 could not last more than 150 cycles at 1C. The occurrence of lithium plating was thus suspected, even when cycling at 25°C. Further work will concentrate on cycling this type of cell at a lower current and/or at a higher temperature.

The Ref#1 showed very different ageing tendencies depending on the cycling temperature. At 25°C, the cells lasted around 800 cycles before reaching the end of first life SOH value. At 0°C, 80 cycles were enough, suggesting the occurrence of lithium plating.

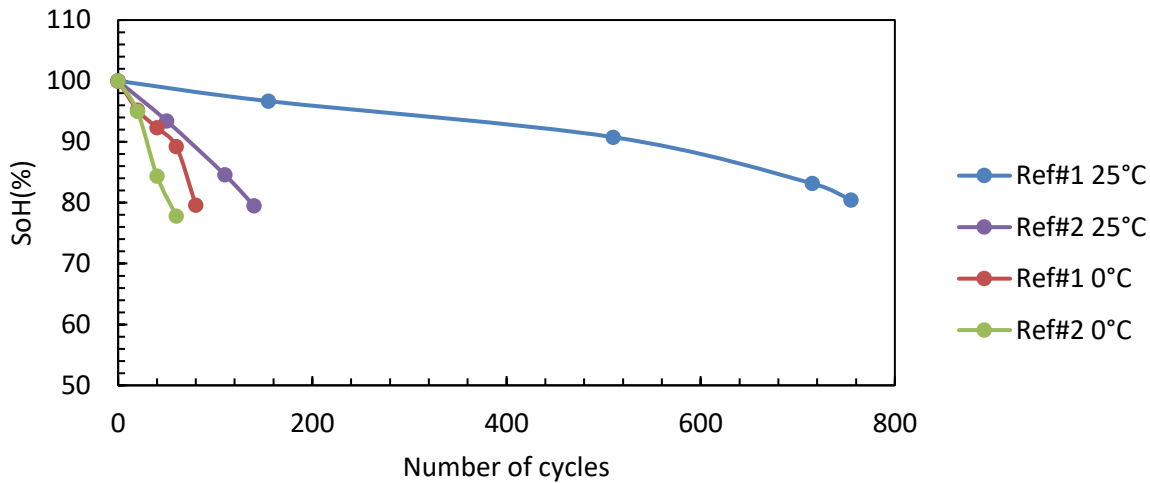


Figure 5: Capacity retention of Ref#1 and Ref#2 while cycling at 0°C or 25°C (charging rate: 1C).

4.1.2 Incremental capacity results

As the capacity fade curves let imagine, the Ref#1 cells suffered from different ageing mechanisms. On Fig. 6, the incremental capacity signal is plotted for two different C-rate, for each ageing temperature. The cyan and the green curves were monitored using the same cell, during the same check-up, at C/2 and C/10 current rate, respectively. For Ref#1, the voltage plateaus at high voltage (highly visible at C/10) are usually attributed to the lithium manganese oxide phase, while the peak at 3,6V (C/10) is attributed to the NMC contribution[6]. Depending on the ageing procedure, we can see that these material do not contribute similarly to the whole capacity of the cell.

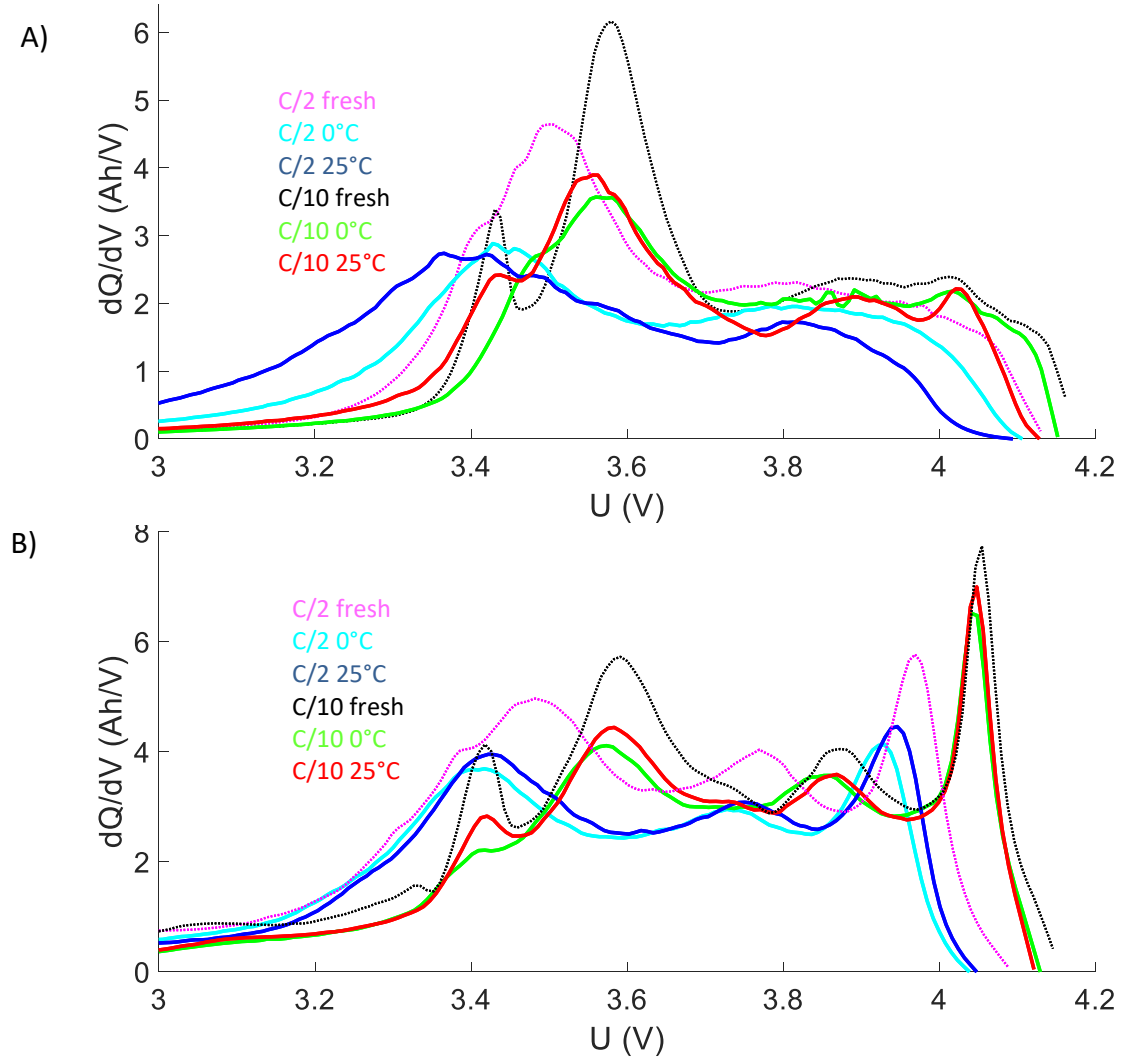


Figure 6: Incremental capacity discharge curves for the Ref#1 (A) and Ref #2 (B), after cycling at 1C, at SOH 100% and 80%. Magenta and black curves are the ICA plots corresponding to the C/2 and C/10 check-up discharges of a fresh cell, respectively; whereas cyan and green curves represents the same check-up steps for a cell at a SOH of 80% cycled at 0°C (check-up was performed at 25°C). Blue and red curves corresponds to a cell at a SOH of 80% cycled at 25°C, C/2 and C/10 discharge check-up, respectively.

When the two different batches of Ref#2 reached a state of health of 80%, it was less easy to see any differences between the two incremental capacity curves, as shown in the Figure 6 B). As the very short lifetime of this cell at 1C suggested, the same degradation mechanism may have affected these cells.

4.1.3 Pulse power characterisations results

Ref#1 cells showed a large increase of their pseudo-resistance calculated by the mean of the charge current pulse, only when they have been cycled at 25°C. The resistance calculated after a pulse of 1s showed a large increase, especially at a low SoC. The pseudo polarisation resistance calculated after a 10s pulse also showed a clear increase. The variations as a function of SoC are depicted in the Figure 7.

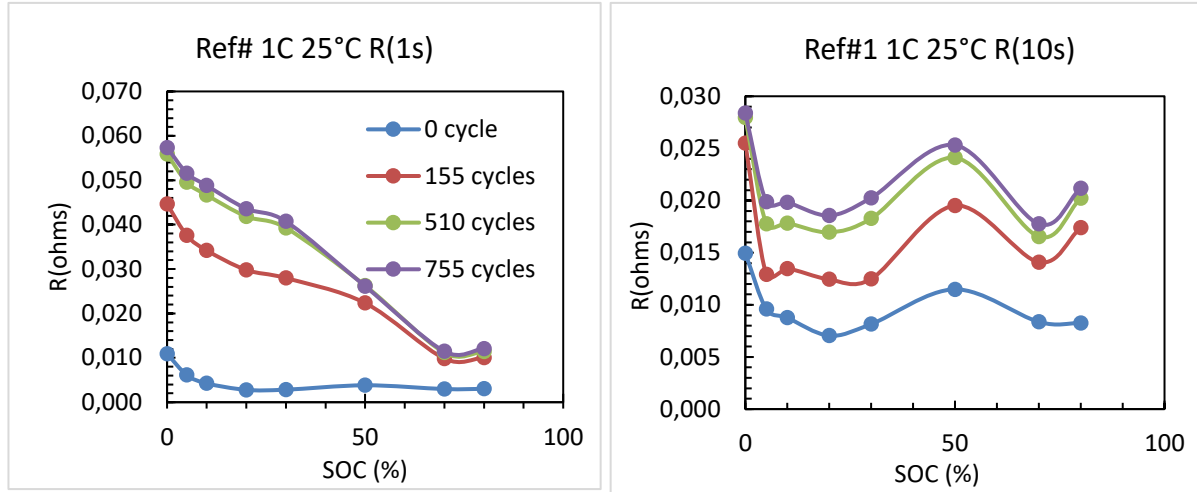


Figure 7: Pseudo-resistance variations when cycling at 25°C. SOH 80% was reached after 755 cycles.

The same reference of cells cycled at 0°C did not show the same variations of resistances as they aged down to SOH 80%, as Figure 8 shows.

For this Ref#1 cells, for a same SOH, the ageing at 0°C led to a very small increase of resistance, while the

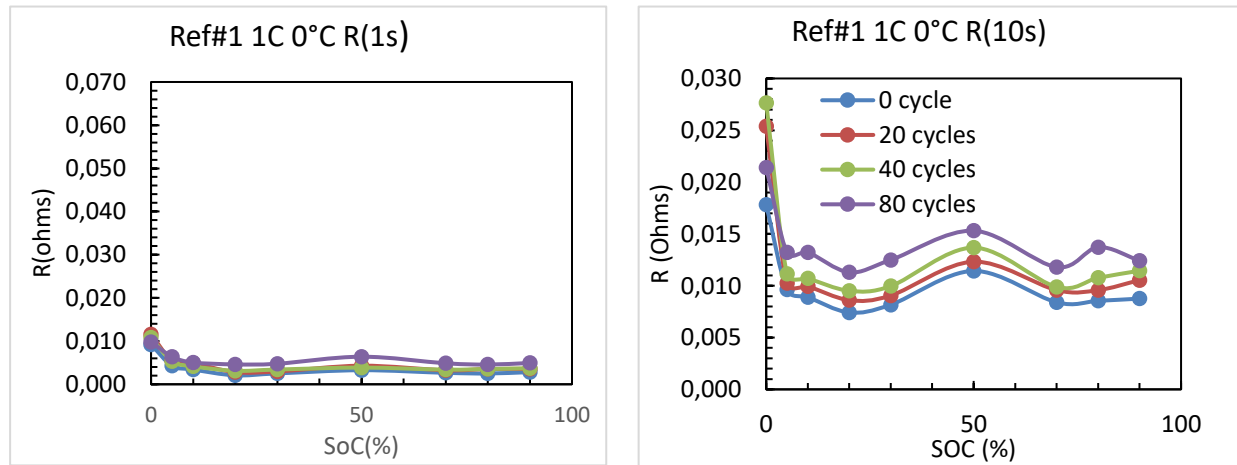


Figure 8: Pseudo-resistances variations when cycling at 0°C. SOH 80% was reached after 80 cycles.

ageing at 25°C showed a much larger increase.

For the Ref#2 pseudo-resistance (not shown here), as observed with the incremental capacity analysis, no difference between the ageing procedures is observed.

4.2 Post-Mortem analysis

4.2.1 Visual aspect and SEM

When dismantling the cell, the degradations turned out to be obvious:

- Ref#1 25°C cycled negative electrode did not stick well to its collector anymore, maybe because it penetrated the separator (black zone). In the parts of the electrode “intact”, some local spots of a white plating were visible and more and more visible towards the core of the winding (Figure 9).



Figure 9: Ref#1 at 80% SoH after cycling at 25°C: the negative electrode (left side) and its copper current collector are visible, while some active material remains stuck to the separator (right side)

- For the three other cells (Ref#1 – 0°C, Ref#2 – 25°C and 0°C), which did not last longer than 150 cycles, white deposition was found on larger areas on the negative electrode, the worst case being the ref#2 cycled at 0°C (Figure 10). The thickness and mass of the electrodes in the white areas have been measured after washing in DMC and drying and the gains were the following : +17µm, +38g/m² for Ref#1 at 0°C; +24µm, +21 g/m² for Ref#2 at 0°C; +28µm, +19g/m² for Ref#2 at 25°C confirming a deposition that could be attributed to lithium-plating as already reported in the literature[7].



Figure 10: a) Ref#2 after cycling 80 cycles at 0°C: a) negative electrode and b) facing separator the silver layer on the electrode is believed to be lithium plating. It is observable that the black zones on the electrodes penetrated the separator

SEM observations showed cracks and a thick layer on the negative electrodes of the three “plated” cells. It was harder to observe the micrometric graphite particles after this plating occurred, as Figure 11 shows.

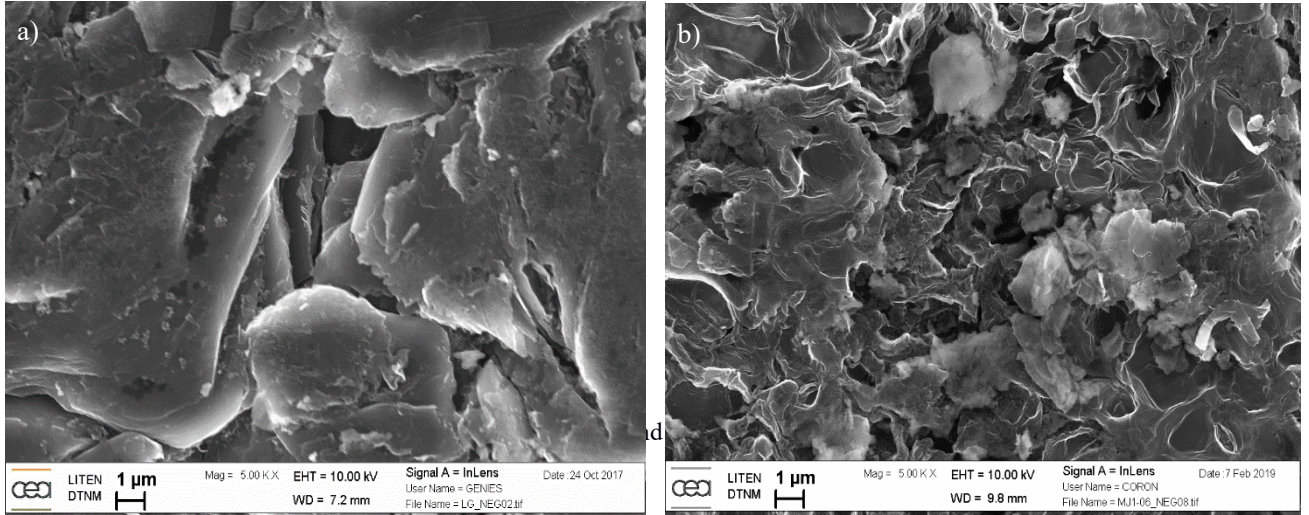


Figure 11: SEM images: Ref#2 negative electrode before (a) and after (b) cycling at 0°C revealing the occurrence of plating.

4.2.2 Half coin-cell cells data

Capacities and residual capacities of the half-cells were measured. It is important to note that the sampling on the negative electrode was done in areas without stronger deposition that can minimize the level of loss of active material. The results are showed in the table 3 and will be completed by data of half coin-cell made of electrode disks with lithium plating.

Table 3: Half-cells results

Ref+Cycling	Electrode	SOH(%)	Residual Capacity (%)
Ref#1 25°C	N	87,5	5
	P	83	
Ref#1 0°C	N	97	19
	P	95	
Ref#2 25°C	N	95	11
	P	99	
Ref#2 0°C	N	94	13
	P	97	

The half coin-cells made of Ref#1-25°C electrodes show that this one suffered from a loss of active materials. The other half coin-cells exhibit a lower loss of active materials, but a higher residual capacity, which is in accordance with the hypothesis of lithium plating. However, as indicated above, it has to be highlighted that the aged electrode are heterogeneous (some zones are more degraded), thus the realisation of half- coin-cell may not be repetitive of the full cell. Further work will focus on the variation of ageing as a function of the location in the cell.

5 Conclusions

Pulse power characterisation which allows calculating pseudo-resistances, appears to be a suitable indicator of the degradation mechanisms. Two cells with the same SOH exhibit very different incremental capacity curves and resistances, thus a comprehensive diagnosis check-up could be based on these tools and is under development. Targeted degradation mechanisms were observed for the Ref#1, i.e. loss of active material

happened after cycling at 25°C. The occurrence of lithium plating was found after cycling at 0°C. However, Ref#2 suffered of plating at both temperatures, warning us about the poor fast charging possibilities of these kind of cells. Lower currents and/or higher temperatures will be necessary to observe loss of active material using this cell. Further work will now be carried out to understand which degradation are prohibitive for a second life, by over-ageing of the studied cells.

References

- [1] E. Martinez-Laserna *et al.*, « Battery second life: Hype, hope or reality? A critical review of the state of the art », *Renew. Sustain. Energy Rev.*, vol. 93, p. 701-718, oct. 2018.
- [2] C. R. Birkl, M. R. Roberts, E. McTurk, P. G. Bruce, et D. A. Howey, « Degradation diagnostics for lithium ion cells », *J. Power Sources*, vol. 341, p. 373-386, févr. 2017.
- [3] M. M. Kabir et D. E. Demirocak, « Degradation mechanisms in Li-ion batteries: a state-of-the-art review », *Int. J. Energy Res.*, vol. 41, n° 14, p. 1963-1986, nov. 2017.
- [4] « (PDF) Incremental Capacity Analysis and Close-to-Equilibrium OCV Measurements to Quantify Capacity Fade in Commercial Rechargeable Lithium Batteries », *ResearchGate*. [En ligne]. Disponible sur: https://www.researchgate.net/publication/230823730_Incremental_Capacity_Analysis_and_Close-to-Equilibrium_OCV_Measurements_to_Quantify_Capacity_Fade_in_Commercial_Rechargeable_Lithium_Batteries. [Consulté le: 12-mars-2019].
- [5] « (PDF) A comparison of methodologies for the non-invasive characterisation of commercial Li-ion cells ». [En ligne]. Disponible sur: https://www.researchgate.net/publication/330369302_A_comparison_of_methodologies_for_the_non-invasive_characterisation_of_commercial_Li-ion_cells. [Consulté le: 11-mars-2019].
- [6] R. Jung, M. Metzger, F. Maglia, C. Stinner, et H. A. Gasteiger, « Oxygen Release and Its Effect on the Cycling Stability of Li_xMn_yCo_zO₂ (NMC) Cathode Materials for Li-Ion Batteries », *J. Electrochem. Soc.*, vol. 164, n° 7, p. A1361-A1377, janv. 2017.
- [7] « Li plating as unwanted side reaction in commercial Li-ion cells – A review ». [En ligne]. Disponible sur: <https://reader.elsevier.com/reader/sd/5F4C6FAF28D1CDD2A3931AAF7A5930AEAFF262A7B632ACECBA18DD0491BB593C7E7BDA547B8ECCD7A20D59B355FDC8B9>. [Consulté le: 08-août-2018].

Author



Eddy CORON

Ph.D. student at the CEA Liten with a material science background. Currently working on the diagnosis of lithium-ion batteries, based on *post-mortem* analysis and modelling.